

Electric Quadrupole Moment of the $^{211}\text{Rn } \frac{63}{2}^-$ Isomer: Absence of Core Deformation at Very High Spins

E. Dafni, M. Hass, E. Naim, and M. H. Rafailovich

Department of Nuclear Physics, The Weizmann Institute of Science, Rehovot 76 100, Israel

and

A. Berger, H. Grawe, and H.-E. Mahnke

*Bereich Kern- und Strahlenphysik, Hahn Meitner Institut für Kernforschung Berlin GmbH,
D-1000 Berlin 39, Germany*

(Received 13 May 1985)

The electric quadrupole moments of ^{211}Rn isomers were determined as $Q(\frac{17}{2}^-) = 19(2) e \cdot \text{fm}^2$ and $Q(\frac{63}{2}^-) = 160(22) e \cdot \text{fm}^2$ via measurements of the quadrupole interaction in a Bi single-crystal host. The results indicate that the spherical shape is preserved in the lead region even at the core-excited very-high-spin regime, in contradiction to theoretical predictions.

PACS numbers: 21.10.Ky, 27.80.+w

The study of high-spin yrast traps in the translead region is of considerable current interest. The occurrence of these isomers is related to the large residual interaction between states with maximum overlap of the nucleonic wave function by alignment of single-particle angular momenta.¹ The concentration of particles in orbitals of high angular momenta at the equatorial plane results in an oblate shape. Calculations with the deformed independent-particle model predict a stable oblate core deformation which increases with increasing spins.²⁻⁴ The predicted effect is most pronounced for very high-spin states involving multi-particle-hole excitation of the lead core. Indeed, reduced slopes of the yrast line at high spins were found for ^{212}Rn ⁵ and ^{211}Rn ⁶ and interpreted as indications for increased effective moments of inertia and hence deformations.

The deformed independent-particle model was successful in reproducing the occurrence and excitation energies of Po, At, and Rn high-spin isomers,³ and its prediction of a deformed core at high spins was borne out in the ^{146}Gd region.^{7,8} On the other hand, the energy depression of core-excited states in Rn nuclei could be accounted for by consideration of only the residual interactions for all states but those with the highest spins.⁹ The two current pictures, of aligned single particles in configurations which are stabilized by the residual interaction and of particles coupled to a deformed oblate core, are not mutually exclusive.^{3,9} Yet a distinction can be made between them as they make very different predictions for the magnitude of the nuclear deformation (see below).

The deformation of core-excited states can best be studied *experimentally* by measurements of the static quadrupole moment Q of the states involved. Q is highly sensitive to the core deformation of high-spin isomers in the lead region because of the high charge and radius of the core, yielding a large intrinsic quad-

rupole moment even for a modest deformation, and because of the high spin of the states for which the measurable spectroscopic moment is very close to the intrinsic moment. To date, quadrupole-moment measurements in the lead region have been limited to moderate-spin states, not involving excitation of the cores; the highest-spin states studied are the $\frac{29}{2}^+$ and 15^- isomers in $^{209,211}\text{At}$ and ^{210}At , respectively.¹⁰ Recently, we have measured the quadrupole coupling constant of the $\pi h_{9/2}^4|_{v=2}$ $^{212}\text{Rn}(8^+)$ isomer in a Bi single-crystal host at 480 K as $e^2 q Q / h = 8.9(4)$ MHz.¹¹ The quadrupole moment was calculated in the shell model from the $8^+ \rightarrow 6^+$ transition rate as $Q(^{212}\text{Rn}(8^+)) = -18(2) e \cdot \text{fm}^2$ (Ref. 11) (including a theoretical uncertainty) resulting in a calibration of the electric-field gradient eq for Rn impurities in Bi. In the present work we have applied the time-differential perturbed-angular-distribution technique to the $\frac{63}{2}^-$ [$E_x = 8.856 + \Delta'$ MeV, $T_{1/2} = 201(4)$ ns]^{12,13} isomer of ^{211}Rn (see Ref. 6 for a level scheme), and the quadrupole moment of the isomer was determined, providing a first direct measurement of the deformation at the very high-spin regime in the lead region. The quadrupole moment of the $\frac{17}{2}^-$ [$E_x = 1.578 + \Delta$ MeV, $T_{1/2} = 596(28)$ ns]⁶ state has also been measured.

The first experiment, employing ^{18}O pulsed beams, were carried out at the 14UD Koffler Pelletron in Rehovot. An isotopically enriched ^{198}Pt target, 0.9 mg/cm² thick, was attached to a Bi single crystal whose \hat{c} axis was perpendicular to the plane, mounted at an angle of 45° to the beam direction, and heated to a temperature of 470 K. ^{211}Rn isomers were populated with use of beams with suitable energy and pulse repetition time: 94 MeV and 1.8 μs for the $\frac{63}{2}^-$ state; 77 and 84 MeV and 3.6 μs for the $\frac{17}{2}^-$ state. Decay γ rays were observed by four large-volume Ge(Li)

TABLE I. Quadrupole moments of Rn isomers.

Isomer	e^2qQ/h (MHz)	$ Q $ ($e \cdot \text{fm}^2$)
$^{212}\text{Rn}(8^+)$	8.9(4) ^a	18(2) ^b
$^{211}\text{Rn}(\frac{17}{2}^-)$		
$E(^6\text{Li})=45 \text{ MeV}$	8.9(7)	
$E(^{18}\text{O})=77 \text{ MeV}$	8.9(5)	
$E(^{18}\text{O})=84 \text{ MeV}$	10.2(5)	
Ave.	9.4(4)	19(2)
$^{211}\text{Rn}(\frac{61}{2}^-)^c$	76(5)	154(21)
$^{211}\text{Rn}(\frac{63}{2}^-)^c$	79(5)	160(22)

^aReference 11.^bA calculated value, Ref. 11.^cTwo alternative spin assignments.

detectors placed at 0° , $\pm 90^\circ$, and 155° (two detectors at 0° and 90° in the $\frac{17}{2}^-$ experiment), and time spectra were accumulated for energy regions of interest. A second similar experiment at the VICKSI combination accelerator in Berlin employed the $^{209}\text{Bi}(^6\text{Li}, 4n)$ reaction (beam energy of 45 MeV; pulse repetition time of $4.16 \mu\text{s}$) to populate the $\frac{17}{2}^-$ isomer in a thick target. This approach yielded improved statistics but a reduced nuclear alignment and no population of the high-spin $\frac{63}{2}^-$ state. As control experiments, we have performed measurements with the crystal's \hat{c} axis directed along the beam, under which conditions no quadrupole perturbation is predicted, and indeed none was found.

After the runs, ratio functions were formed from the normalized background-subtracted time spectra at 0° (and 155°) and 90° :

$$R(t) = \frac{Y(0^\circ, t) - Y(90^\circ, t)}{Y(0^\circ, t) + Y(90^\circ, t)}.$$

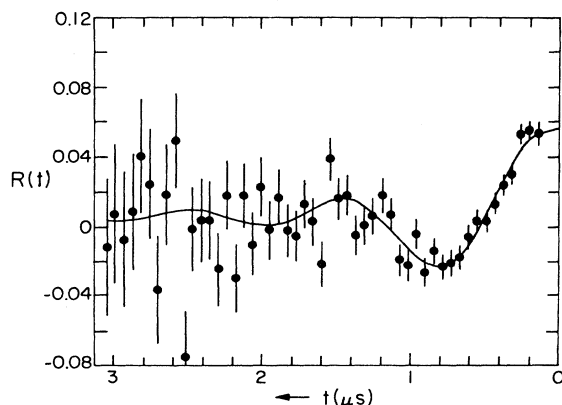


FIG. 1. Ratio function for the 540- and 918-keV γ transitions from the decay of the $^{211}\text{Rn}(\frac{17}{2}^-)$ isomer. The solid line is from a two-level fit (see text and Ref. 11), including the effect of the $\frac{13}{2}^-$ state.

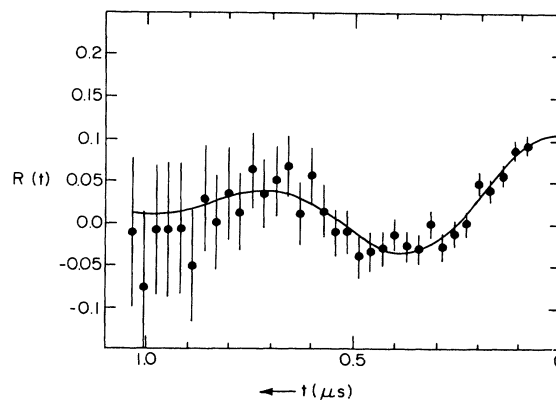


FIG. 2. Ratio function and a fit for the 687 and 1299 $E3$ transitions from the decay of the higher-spin isomer in ^{211}Rn ; a spin assignment of $\frac{63}{2}^-$ is assumed.

In the case of the higher-spin isomer, $R(t)$ was fitted by a theoretical expression assuming a quadrupole perturbation to a single isomer¹⁴ which yields directly the value of the quadrupole coupling constant e^2qQ/h . Alternative spin assignments were considered: $\frac{61}{2}^-$ as believed earlier⁶ and $\frac{63}{2}^-$ as adopted recently.^{12,13} In the case of the $\frac{17}{2}^-$ isomer, we have applied a two-level fitting procedure,¹¹ taking into account the effect of the finite mean life of the $\frac{13}{2}^-$ level. Fixed values of $\tau_{13/2} = 80 \text{ ns}$, sidefeeding of 20% directly to the $\frac{13}{2}^-$ state, and $Q(\frac{17}{2}^-)/Q(\frac{13}{2}^-) = 5$ were assumed; however, the results were insensitive to small variations in these parameters. The fitting results are listed in Table I, and some of the data are shown in Figs. 1 and 2. Using the measured quadrupole coupling constants for $^{212}\text{Rn}(8^+)\text{Bi}$ and the calculated value of $Q(^{212}\text{Rn}(8^+))$ (Table I), we arrive at the values of quadrupole moments listed in Table I.

The similarity between the quadrupole coupling constants of $^{212}\text{Rn}(8^+)$ and $^{211}\text{Rn}(\frac{17}{2}^-)$ is expected: The two isomers have the same $\pi h_{9/2}^4 |v=2$ structure with the addition of a $p_{1/2}$ neutron hole to the $\frac{17}{2}^-$ state, which does not affect the quadrupole moment to first order. A shell-model calculation of the quadrupole moment of the high-spin isomer was carried out for several proposed configurations^{6,12} for a total assumed

TABLE II. Single-particle moments in the lead region.

	Orbital	Q_{sp} ($e \cdot \text{fm}^2$)	Reference
Protons	$h_{9/2}$	-43	15
	$i_{13/2}$	-62	16
Neutrons	$f_{5/2}^{-1}$	+20	16
	$g_{9/2}$	-29	17
	$i_{11/2}$	-28	16
	$j_{15/2}$	-42	16

TABLE III. Shell-model quadrupole moments.

I^π	Configuration	Q ($e \cdot \text{fm}^2$)
$\frac{61}{2}^-$	$\pi(h_{9/2}^2 i_{13/2}^2)_{20} + \nu(p_{1/2}^{-1} f_{5/2} j_{15/2})$	-175
$\frac{63}{2}^-$	$\pi(h_{9/2}^2 i_{13/2}^2)_{20} + \nu(f_{5/2}^{-1} g_{9/2} i_{11/2})$	-214
$\frac{63}{2}^-$	$\pi(h_{9/2}^3 i_{13/2})_{17} - \nu(f_{5/2}^{-1} i_{11/2} j_{15/2})$	-186
$\frac{63}{2}^-$	$\pi(h_{9/2}^3 i_{13/2})_{17} - \nu(f_{5/2}^{-1} g_{9/2} j_{15/2})$	-162

spin of $\frac{61}{2}$ and $\frac{63}{2}$. The single-particle quadrupole moments used in these calculations are listed in Table II and the results are given in Table III; similar results are expected for other possible configurations or for a mixed wave function.¹² The results demonstrate that the experimental value of $|Q(\frac{63}{2}^-)|$ can be explained within the spherical shell model, with little sensitivity to details of the single-particle configurations assumed.

An alternative way, more closely related to the deformed independent-particle model, of computing Q is by consideration of the contribution of the deformed core explicitly rather than via effective charges⁸:

$$Q = f(I)Q_0 = f(I)(Q_i + Q_{\text{core}}),$$

where $f(I) = I(2I-1)/(I-1)(2I-3)$, Q_i is the quadrupole moment of the bare valence particles ($e_{\text{eff}} = 1$ for protons, 0 for neutrons), and for an axially symmetric uniformly charged core,

$$Q_{\text{core}} = (3/\sqrt{5}\pi)Z_{\text{core}}R^2(\beta + 0.36\beta^2).$$

Q_i were calculated with use of $\langle r^2 \rangle$ values of 34.8 and 41.7 $e \cdot \text{fm}^2$ for the $h_{9/2}$ and $i_{13/2}$ proton orbitals, respectively,¹⁸ and Q_{core} was calculated with $R = 1.12 \times A_{\text{core}}^{1/3}$. The calculated values of Q as a function of β are shown in Fig. 3 for the configurations

$$\{\pi h_{9/2}^4 |_{\nu = 2\nu p_{1/2}^{-1}}\} \frac{17}{2}^-$$

and

$$\{\pi(h_{9/2}^2 i_{13/2}^2)_{\nu}(f_{5/2}^{-1} g_{9/2} i_{11/2})\} \frac{63}{2}^-;$$

other $\frac{63}{2}^-$ configurations yielded essentially the same result. Also shown are the experimental values with the signs of the quadrupole moments assumed to be negative (the signs are not measured with the present technique). From Fig. 3 a value of $\beta = -0.03(1)$ is deduced for the $^{211}\text{Rn}(\frac{63}{2}^-)$ level, ruling out any significant core deformation.

In contradiction to the present experimental result the deformed independent-particle model predicts $\beta \approx 0.1$ for the $^{212}\text{Rn}(30^+)$ isomer.²⁻⁴ Core-excited isomers in the $N = 125$ ^{209}Po and ^{210}At nuclei are calculated to have similar deformations to the corresponding isomers in the $N = 126$ ^{210}Po and ^{211}At nuclei.³ Therefore, the prediction for $^{212}\text{Rn}(30^+)$ is

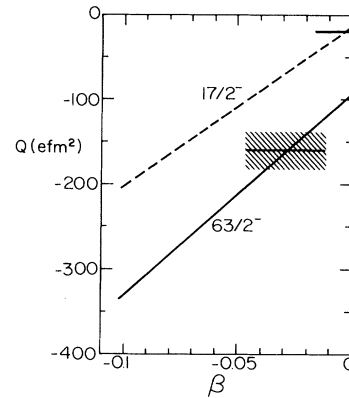


FIG. 3. Calculated quadrupole moments in the deformed independent-particle picture as a function of the deformation. Also shown are the present experimental results.

probably relevant also for the closely related $^{211}\text{Rn}(\frac{63}{2}^-)$ state. The participation of an aligned neutron hole at a high- j orbital (i.e., $i_{13/2}^{-1}$) in the $^{211}\text{Rn}(\frac{63}{2}^-)$ single-particle configuration, which could reduce the predicted deformation,³ is ruled out since such a configuration will not be isomeric because of the repulsive proton-neutron hole interaction in a stretched coupling.^{3,9}

In conclusion, the present measurement of $Q(^{211}\text{Rn}(\frac{63}{2}^-))$ does not confirm the deformation of core-excited isomers in the translead region, predicted by the deformed independent-particle model. It demonstrates that the spherical shape is preserved in the ^{208}Pb region even at the very high-spin core-excited regime. The view that high-spin isomerism in the lead region is due to attractive residual interactions, rather than deformation energy, is supported.

¹A. Faessler, M. Ploszajczak, and K. R. S. Devi, Phys. Rev. Lett. **36**, 1028 (1976).

²C. G. Andersson, G. Hellström, G. Leander, I. Ragnarsson, S. Åberg, J. Krumlinde, S. G. Nilsson, and Z. Szymanski, Nucl. Phys. **A309**, 141 (1978).

³K. Matsuyanagi, T. Døssing, and K. Neergård, Nucl. Phys. **A307**, 253 (1978).

⁴J. Dudek, Z. Szymanski, and T. Werner, Phys. Rev. C **23**, 920 (1981).

⁵D. Horn, O. Häusser, T. Faestermann, A. B. McDonald, T. K. Alexander, J. R. Beene, and C. J. Herrlander, Phys. Rev. Lett. **39**, 389 (1977); D. Horn, O. Häusser, T. Faestermann, H. R. Andrews, and D. Ward, Nucl. Phys. **A317**, 520 (1979).

⁶A. R. Poletti, G. D. Dracoulis, C. Fahlander, and I. Morrison, Nucl. Phys. **A359**, 180 (1981); G. D. Dracoulis, C. Fahlander, and A. R. Poletti, Phys. Rev. C **24**, 2386 (1981).

⁷T. Døssing, K. Neergård, and H. Sagawa, J. Phys. (Paris), Colloq. **41**, C10-79 (1980).

⁸O. Häusser, H.-E. Mahnke, T. K. Alexander, H. R. Andrews, J. F. Sharpey-Schafer, M. L. Swanson, and D. Ward, Nucl. Phys. **A379**, 282 (1982).

⁹A. P. Byrne and G. D. Dracoulis, Nucl. Phys. **A391**, 1 (1982).

¹⁰H.-E. Mahnke, W. Semmler, H. Grawe, H. Haas, and R. Sielemann, Phys. Lett. **122B**, 27 (1983).

¹¹E. Dafni, M. Hass, E. Naim, M. H. Rafailovich, A. Berger, H. Grawe, and H.-E. Mahnke, Nucl. Phys. **A441**, 501 (1985).

¹²A. R. Poletti, G. D. Dracoulis, A. P. Byrne, A. E. Stachbery, S. J. Poletti, J. Gerl, and P. M. Lewis, Phys. Lett. B (to be published).

¹³We adopt here the recent spin assignment $\frac{63}{2}$ for the

high-spin isomer in ²¹¹Rn following Ref. 12, rather than the previous assignment (Ref. 6).

¹⁴E. Dafni, R. Bienstock, M. H. Rafailovich, and G. D. Sprouse, At. Data Nucl. Data **23**, 315 (1976).

¹⁵G. Astner, I. Bergström, J. Blomqvist, B. Fant, and K. Wikström, Nucl. Phys. **A182**, 219 (1972).

¹⁶D. J. Donahue, O. Häusser, R. L. Hershberger, R. Lutter, and F. Riess, Phys. Rev. C **12**, 1547 (1975).

¹⁷D. J. Decman, J. A. Becker, J. B. Carlson, R. G. Lanier, L. G. Mann, G. L. Struble, K. H. Maier, W. Stöfl, and R. K. Sheline, Phys. Rev. C **28**, 1060 (1983).

¹⁸J. Blomqvist and S. Wahlborn, Ark. Fys. **16**, 545 (1960). $\langle r^2 \rangle$ values were calculated from the radial wave functions given in Appendix B.